Journal of Non-Crystalline Solids: X 6 (2020) 100049

Contents lists available at ScienceDirect

Journal of Non-Crystalline Solids: X

journal homepage: www.journals.elsevier.com/journal-of-non-crystalline-solids-x

Anionic speciation in sodium and potassium silicate glasses near the metasilicate ($[Na,K]_2SiO_3$) composition: ^{29}Si, ^{17}O, and ^{23}Na MAS NMR

Jonathan F. Stebbins

Department of Geological Sciences, Stanford University, Stanford, CA 94305, USA

ARTICLE INFO

Keywords:
Nuclear magnetic resonance
Silicate glass structure
Oxygen speciation
Sodium metasilcate
Potassium carbonate

ABSTRACT

Alkali silicate glasses near to the metasilicate composition provide sensitive tests of anionic speciation. However, reports on ^{29}Si NMR data vary considerably in their derived proportions of silicate species. In some cases, an apparent deficit in the content of non-bridging oxygen has been attributed to up to 5 to 10% "free" oxide ions. Here we provide new NMR data on a series of sodium silicate glasses ranging from 56 to 45 mol% silica with accurately analyzed compositions. High signal-to-noise data for a ^{29}Si-enriched glass provide improved constraints on fitting models for spectra, and suggests a slight asymmetry in the main Q^2 component. Data are consistent with conventional models in which "free" oxide contents are below detection limits of about 0.5 to 1%. Spectra for an ^{17}O-enriched K-silicate glass with about 53% silica confirm that there is no obvious direct signature for "free" oxide species in this compositional range.

1. Introduction

Binary alkali silicate glasses, for example those in the Li_2O-SiO_2, Na_2O-SiO_2 and K_2O-SiO_2 systems, have been widely studied by diffraction and spectroscopic methods for many decades, as they are often considered to simply represent many of the structural questions that control their properties as well as those of more complex compositions [1,2]. They also have relatively wide and accessible regions of glass formation, between those at high silica content where phase separation occurs (Na- and Li-silicates) and low silica content where crystallization and alkali volatility become problematical. Although the binary compositions themselves are generally too water-sensitive to have many technological applications, roughly 50–50 mixtures of sodium and calcium silicate components comprise the bulk of "soda-lime" glasses that are so widely used in conventional glass containers and windows. Somewhat surprisingly, there remain incompletely resolved, fundamentally important, questions concerning the structure of the silicate anionic network in alkali silicate glasses and liquids.

Among the best-studied aspects of structural order/disorder in silicate glasses is the distribution of bridging and non-bridging oxygens (BO and NBO) among the network-forming SiO_4 groups. At the shortest length scale this can be characterized by concentrations of "Q^n" groups, with n representing the number of bridging oxygens in a given tetrahedron, 4–n the number of NBO, and Q stemming from "quaternary". Many models of glass and liquid structure describe such distributions in terms of equilibria among such species (for $n = 1$, 2 or 3):

$$2Q^n \Longleftrightarrow Q^{n-1} + Q^{n+1} \quad (1)$$

Alkali silicate glasses are nearly unique in having at least partially resolvable contributions from such species in ^{29}Si MAS NMR. From some of the earliest studies of silicate glasses by this method in the early 1980's [3–10], the inherently quantitative relationship in NMR between concentration and signal intensity has been applied to measure relative abundances of Q^n groups and to constrain the energetic and entropic consequences of equilibria such as [1]. This method has particularly complemented older but still ongoing studies by Raman spectroscopy of such glasses, which although complicated by possible variation in absorption cross section with composition and structure, also often show relatively well-resolved features for Q^n species [1,11–17]. Alkali silicate (and other) glasses also often have partially resolvable components for the bridging and nonbridging oxygens in ^{17}O MAS NMR and oxygen 1 s XPS spectra, providing additional complementary data on this aspect of the structure [18,19].

An even more fundamental aspect of the anionic structure is captured by the reaction that in itself is relied upon to synthesize many silicates, both crystalline and glassy, namely the combination of a "modifier" oxide (e.g. alkali, alkaline earth, and most transition metal oxides) with silica to distribute the oxygen anions among bridging and non-bridging oxygens and any unreacted "free" oxide ions (not coordinated by any Si: also labeled as "metal bridging oxygen", MBO in some studies [20]):

$$FO + BO \Longleftrightarrow 2\,NBO \quad (2)$$

E-mail address: stebbins@stanford.edu.

https://doi.org/10.1016/j.nocx.2020.100049
Received 10 February 2020; Received in revised form 10 March 2020; Accepted 12 March 2020
Available online 24 March 2020

In silicates with O/Si > 4 (i.e. lower silica than the Q^0 or orthosilicate stoichiometry M_4SiO_4), excess free oxide must be present if all Si is four-coordinated. Equilibria of all three oxide species have long played a key role in descriptions of low-silica slags of critical importance in extraction and refining of metals [21,22]. In contrast for higher-silica liquids, which include nearly all glass-forming compositions, most models make the approximation that FO concentrations are low enough to be negligible for properties of interest, as well as in the analysis of spectroscopic data. However, recent interpretations of oxygen 1 s XPS data on alkali silicates (in which NBO and BO contents were estimated by fitting spectra and FO contents deduced from the glass composition by mass balance), combined with reinterpretation of published as well as some new NMR data, have suggested that FO may be present at the several percent level in K- and Na-silicate glasses as rich in silica as 60% to 70% SiO_2 [20,23–26].

High alkali silicate glasses represent key tests of this question, as such compositions maximize possible FO concentrations, and narrow the compositional gap between observable glass structures and models of low-silica slag chemistry, which are generally based solely on thermodynamics of high-temperature solid-liquid-vapor phase equilibria. Although such glasses pose significant experimental challenges in terms of compositional control (alkali volatilization, carbonate retention from starting materials, extreme hygroscopicity), sodium and potassium silicates glasses can be readily formed in small batches up to about 50 to 55 mol% alkali oxide. Remarkable and importantly, lithium silicate glasses have been formed by roller quenching to as high as 64% Li_2O and analyzed in detail by NMR [27].

Compositions close to the metasilicate (e.g. Na_2SiO_3, 50% Na_2O) are especially critical as being near the edge of the normal glass-forming range, and in having Q^n species that vary sensitively with composition around the average of Q^2. Speciation deduced from spectroscopy, and resulting models of structure, will depend on careful evaluations not only of models used to fit the data, but on precise and accurate compositional analyses. Taking advantage of the availability of a sample of crystalline sodium metasilicate, synthesized from 95% isotopically enriched silica [28], as well as a range of isotopically normal Na-silicates, this study takes a closer look at anionic speciation and attempts to find consistency among somewhat disparate previous data sets. In addition, we examine the constraints on such speciation using ^{17}O MAS NMR on a K-silicate glass of similar composition.

2. Experimental methods

2.1. Sample syntheses

Glasses of nominal Na_2SiO_3 composition were made by melting three different crystalline sodium metasilicate (NMS) starting materials. The first of these (NMS-A) was synthesized in large (ca. 20 to 100 g) batches from Na_2CO_3 and SiO_2, followed by crystallization at 800 °C, as part of a previous NMR study of this phase [28]. ^{29}Si NMR and ^{23}Na NMR showed only the NMS phase (see below), indicating close to ideal composition. A second glass was made by melting a 95% ^{29}Si-enriched crystalline NMS sample also from that earlier study [28], which contained about 2% $Na_2Si_2O_5$ phases as detected by ^{29}Si MAS NMR and thus an estimated bulk composition of about 49.7 ± 0.5% Na_2O. Both of these NMS samples were coarsely crystalline and broke into narrow elongated fragments when crushed, as previously described [28,29]. A third glass was made by melting sodium metasilicate reagent, NMS-rg (Sigma-Aldrich), for which ^{29}Si NMR and ^{23}Na NMR both indicated a small amount of silicates with Na/Si > 2 and thus a slight excess in Na_2O over stoichiometry. This reagent consisted of uniformly-sized spheres (ca. 0.1 mm) comprised of very small crystallites, which needed no crushing prior to collection of NMR data. Glasses were made by melting 1 to 2 g batches for about 1 h at 1200 °C to 1360 °C in Pt-3% Au crucibles, then quenching rapidly by dipping the bottom of the crucible in water (Table 1). Sample weights were monitored and indicated a slight loss of Na_2O during melting.

Glasses of nominal composition 47 and 44 mol% Na_2O were made by mixing fine-grained amorphous silica (silicic acid dehydrated at 900–1000 °C) with NMS-A and melting and quenching as above; glasses of nominal compositions 52.5 and 55 mol% Na_2O were made by addition of Na_2CO_3 to NMS-A and melting as above. All glasses were optically clear, free of bubbles, and showed no evidence for crystallinity in either ^{29}Si or ^{23}Na MAS NMR spectra.

Because of well-known greater separation of ^{17}O chemical shifts in comparison to the Na_2O-SiO_2 system [30], four glass samples of nominal K_2SiO_3 composition were synthesized from K_2CO_3 combined with either isotopically normal SiO_2 or about 60% ^{17}O-enriched SiO_2 as previously described [31]. One glass of each starting mixture was melted for about 1 h at 1200 °C, a second at 1300 °C. ^{17}O-enriched K_2CO_3 (used for comparing spectra, not for glass synthesis) was formed by dissolving 0.1 g of K_2CO_3 reagent in 0.6 g of 20% ^{17}O-enriched H_2O, allowing several days for equilibration in a sealed tube, then successively drying at 60, 115, and 250 °C in air.

All of the glasses synthesized here had about 0.1 to 0.2 wt% added cobalt oxide to speed spin-lattice relaxation, which is known from previous work to have a negligible effect on structure or lineshapes when phase separation is not present (the latter occurs in this system only at much higher silica contents). Glasses were a typical dark blue in color from tetrahedrally-coordinated Co^{2+}, except for those with > 50% Na_2O, which were a darker, brownish green color. This may be due to dissolution of traces of Au or Pt from the crucibles in these relatively corrosive compositions, or, conceivably, to some change in the bonding environment of cobalt cations.

Especially for the glasses of 47% and higher alkali oxide content, samples were deliquescent, absorbing H_2O from normal laboratory air and, for small fragments, converting to aqueous solutions or gels within minutes to hours. To eliminate this problem, each glass was immediately transferred to a desiccator after melting and was stored as large fragments, sealed in plastic tubes with o-ring closures, over P_2O_5; samples were coarsely crushed for chemical analysis or for loading into MAS NMR rotors, all in a glove box flushed with dry nitrogen. No changes in the weights of the loaded rotors were detected even after four days of NMR data collection; preliminary spectra collected for a few hours at the beginning of experiments on a given sample matched those collected at the end of acquisition–both indicating that water absorption in rotors was negligible.

2.2. Chemical analyses

All of the glasses made here were readily soluble in water, greatly facilitating analysis by simple 'wet' chemical methods. One to three large fragments of each glass, totaling 25–50 mg, were rapidly weighed, dissolved together in 25–30 mL of deionized water, then titrated with dilute sulfuric acid ('standardized solutions,' Alfa Aesar) using methyl orange as the end point indicator [32,33]. This standard method for sodium metasilicate yields a precise and accurate measure of Na_2O or K_2O. 5 samples of each isotopically normal glass were analyzed, yielding standard deviations of about 0.1 to 0.3% absolute (Table 1). The method was tested on Na_2CO_3 and on crystalline Na_2SiO_3 yielding results within about 0.3 to 0.4% (absolute) of ideal alkali content. We thus report the uncertainty of this analysis to ± 0.5% (absolute, e.g. 49.5 ± 0.5% Na_2O). The ^{29}Si and ^{17}O-enriched glasses were not analyzed, given their cost, but compositions were estimated by comparisons of ^{29}Si NMR spectra with those for analyzed samples (see below).

"Retained" CO_2, which could be a potential problem in high alkali silicate glass synthesis [34,35], is presumably negligible in the 50% Na_2O, 47% and 44% Na_2O glasses, as carbonate was not added during their preparation. For the nominally 50% K_2O glasses, however, which were made by more standard methods from silica and alkali carbonate, NMR spectra for the ^{17}O-enriched glass melted at 1200 °C clearly

Table 1
Glass compositions, peak heights, and representative results of fitting exercises for ^{29}Si MAS NMR spectra.

					fit 1[d]				fit 2[e]					
Name	%Na_2O nom.[a]	T, °C	%Na_2Omeas.[b]	Q^1/Q^2 height[c]	Q^0	Q^1	Q^2	Q^3	Q^0	Q^1A	Q^1B	Q^2A	Q^2B	Q^3
N50-en[f]	50.0	1200	49.2	0.200		*9.9*	*72.4*	*17.8*		10.2		58.7	16.0	15.1
N50–1	50.0	1360	49.8	0.227		*10.4*	*72.1*	*17.5*		11.3		49.9	25.2	13.6
N50–2	50.0	1200	49.7	0.230		*11.2*	*71.7*	*17.2*		11.7		56.6	17.0	14.7
N50–3[g]	50.0	1200	50.9	0.370		*17.7*	*70.3*	*12.0*		18.0		59.6	12.7	9.7
N55–2	55.0	1200	54.7	1.130	1.5	39.2	54.8	4.5	*2.2*	*32.6*	*9.3*	*49.7*		*6.3*
N55–3	55.0	1300	54.8	1.090	1.2	38.7	54.4	5.7	*1.6*	*36.1*	*3.6*	*55.4*		*3.3*
N525	52.5	1200	52.2	0.508		23.2	66.9	9.8	*1.5*	*22.6*		*66.4*		*9.5*
N47	47.0	1300	46.7	0.115		*4.8*	*63.3*	*31.9*		5.3		47.2	17.3	30.2
N44	44.0	1300	43.7	0.060		*1.9*	*50.4*	*47.7*		2.0		41.0	10.1	46.9
K50	50.0[h]	1300	47.3[h]											
K50	50.0[h]	1200	–											

[a] Nominal composition in mole %.
[b] Mole % measured by titration, except for N50-en, which was estimated from NMR peak height data in Fig. 5; uncertainties are roughly ± 0.5% (absolute).
[c] Relative peak heights measured directly from spectra without fitting.
[d] Percent areas, fits with single Gaussian component for each species.
[e] Fits with extra Q^1 or Q^2 peak to test peak asymmetry; preferred results are in normal font and are plotted in Fig. 9; less preferred results in italics.
[f] Made by melting NMS (crystalline Na_2SiO_3) that was isotopically enriched to ca. 95% ^{29}Si.
[g] Synthesized using commercial NMS reagent; others with NMS from previous study (see text).
[h] Mole % K_2O.

showed the presence of about 0.7% oxygen as carbonate, based on new data for ^{17}O-K_2CO_3 (see below). This was completely removed on re-melting at 1300 °C, however, accompanied by a significant change in the ^{29}Si NMR spectrum of the isotopically normal analog sample. For the nominally 55% Na_2O glass (made with a small amount of added Na_2CO_3), no significant differences in the ^{29}Si spectra were noted for 1200 °C vs. 1300 °C melting, indicating that CO_2 retention was unlikely to be significant for this synthesis route for this composition.

2.3. NMR spectroscopy

All NMR spectra were collected with a Varian Infinity 600 spectrometer (14.1 Tesla field), using a Varian/Chemagnetics "T3" MAS probe and 33 μL volume zirconia rotors usually spinning at 14 kHz. Some ^{29}Si spectra were collected at slower spinning rates to facilitate comparison with previously published data. Sample weights were typically 30 to 45 mg. ^{29}Si spectra (119.2 MHz) were referenced to tetramethylsilane (TMS) at 0 ppm; ^{23}Na spectra (158.8 MHz) to 1 *m* aqueous NaCl at 0 ppm (crystalline NaCl was measured at 7.2 ppm) and ^{17}O spectra (81.3 MHz) to 20% ^{17}O H_2O at 0 ppm. Most ^{23}Na spectra were collected with the same rotors and spinning rate; ^{17}O spectra were collected with smaller inside diameter rotors and spinning rates to 23 kHz. For all nuclides, single pulse acquisition was used with radio-frequency tip angles of about 30° or less; Gaussian apodization was applied to optimize signal to noise ratio (S/N) without causing measurable line broadening. A linear prediction algorithm was applied to original time-domain data to back-predict through the approximately 20 μs of instrumental deadtime, ensuring flat baselines.

Spin lattice relaxation was relatively rapid for the glasses because of the Co^{2+} dopant. ^{29}Si spectra were acquired at pulse delays of 1 to 60 s. No differential relaxation was seen (difference in peak shape as a function of delay time); most spectra shown were acquired at an optimal S/N at a delay of 4 s to 20 s and typically 4000 to 40,000 signal averages. In contrast, relaxation of the crystalline Na_2SiO_3 samples studied here was much slower, often at least minutes, apparently because of the lack of substitution of paramagnetic transition metals into the crystal structure. Relaxation for the quadrupolar nuclides ^{23}Na and ^{17}O in the glasses was typically very rapid, allowing spectra to be acquired with pulse delays of 0.1 to 1 s.

2.4. Fitting of ^{29}Si spectra

^{29}Si spectra were fitted using least-squares regression (VNMRJ software) and a minimal number of components. Initial analyses of the spectra for the isotopically enriched N50 glass (N50-en), for which signal-to-noise ratios of about 1500 were readily obtainable, clarified details of line shapes, widths, and number of detectable components that were then applied to lower S/N data (ca. 80–120) for isotopically normal glasses. 100% Gaussian component shapes were clearly the best approximation. In particular for the predominant Q^2 peak, a slight asymmetry was detected that was best reproduced by adding a second, smaller Q^2 component to the fit, significantly improving the quality of the fits. For low intensity components in some compositions (e.g. Q^3 in the higher-Na glasses and Q^1 in the lower-Na glasses), component widths were constrained by results for compositions in which these peaks were larger.

3. Results and discussion

3.1. ^{29}Si spectra: Effects of composition and melting temperature

Representative ^{29}Si MAS NMR spectra for isotopically normal Na-silicate glasses are shown in Fig. 1, data for the ^{29}Si-enriched N50-en glass in Figs. 2 and 3, and for the K50 glasses in Fig. 4. For the Na-silicates, clearly visible are partially resolved components that have long been assigned to different Q^n species. As expected, for compositions near to 50% Na_2O, the predominant component is that for Q^2, as in the corresponding structure of crystalline Na_2SiO_3, which has a single NMR peak at −76.8 ppm [28]. In the glasses, this peak maximum increases slightly in frequency from −76.5 ± 0.2 ppm in N44 to −75.3 ppm in N55, as has been observed previously in studies of much wider compositional ranges [23,36].

The relative proportions of the next-most abundant components (Q^1 and Q^3) vary dramatically around the N50 composition. This is particularly obvious in comparison of the relative heights of the two narrower, better-resolved peaks (Q^1 and Q^2), for example the clear

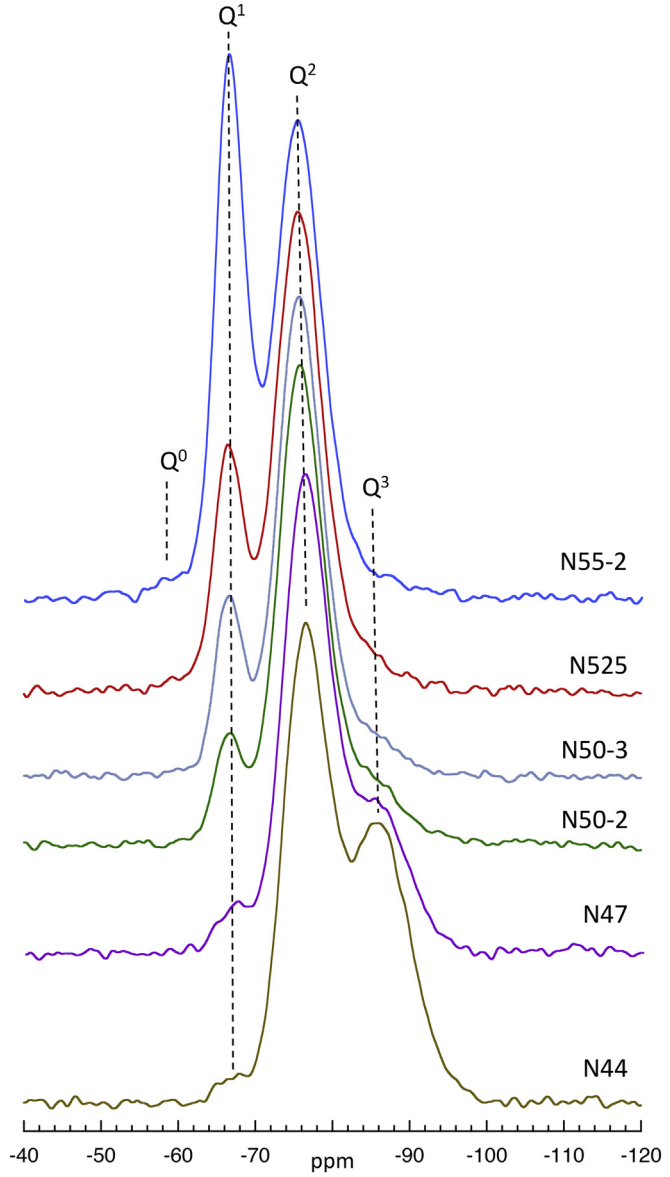

Fig. 1. ^{29}Si MAS NMR spectra of sodium silicate glasses with natural isotopic abundance. Sample numbers are based on nominal compositions: analyzed compositions are slightly different (see Table 1). Here and in Figs. 2 and 3, intensities are normalized to that of the central Q^2 peak.

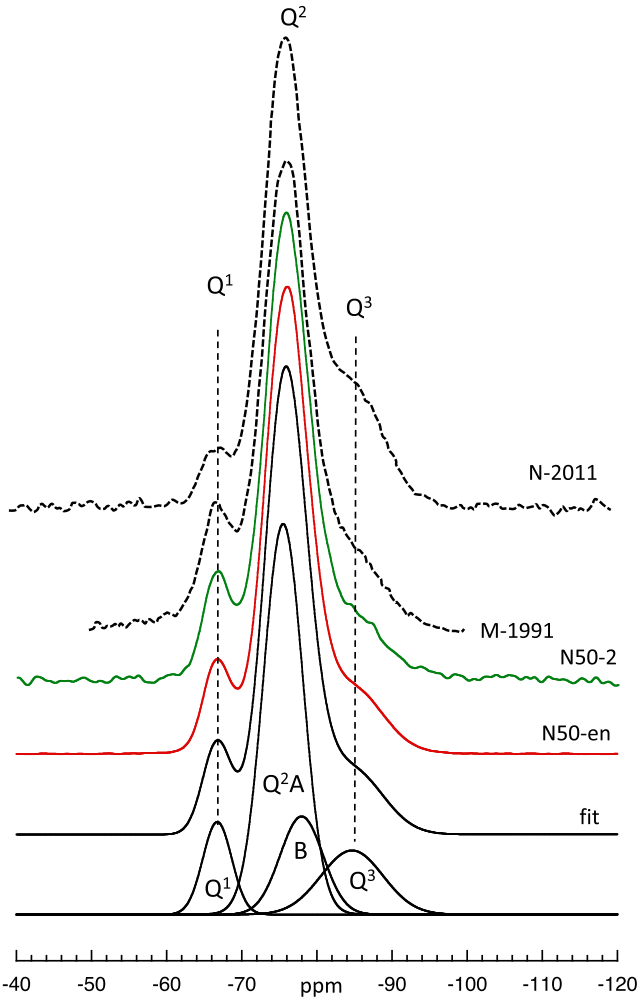

Fig. 2. ^{29}Si MAS NMR spectra of sodium silicate glasses with close to 50 mol% Na_2O, comparing data from this study for one of the natural abundance (N50–2) glasses and the isotopically enriched (N50-en) glass (see Table 1 for actual compositions). The preferred, four-peak fit as described in text is shown for the latter. Also shown are published spectra from two glasses of the same nominal composition: 'M-1991' from [36], 'N-2011' from [23].

difference in peak heights made by an increase of only 1.2% in Na_2O from sample N50–2 to N-50-3 (Fig. 1 and Table 1). Measured ratios of peak heights Q^1/Q^2 vs. analyzed compositions are shown in Fig. 5 and demonstrate a systematic variation with composition in this range, independent of any fitting of spectra. The correlation is, as expected, non-linear. A thermodynamic distribution based on the actual concentrations of Q^n species (see below) would give a similarly-shaped curve, for example, but one that would not be identical because of effects of peak overlap on measured heights.

Within this relatively narrow range of compositions, this Q^1/Q^2 peak height relationship can be used to estimate the compositions of Na-silicate glasses for which accurate compositional analyses are not available. For example, the ^{29}Si-enriched N50-en glass in this study (not analyzed because of the cost of the isotope), although nominally of 50% Na_2O, clearly has a lower actual alkali content, estimated as 49.2 ± 0.5%. The 50% Na_2O glass in a widely-cited early, systematic study of alkali silicates [36] appears to be close to its nominal composition, but its spectrum may be subject to some slight lineshape distortions typical of early, relatively low-field (4.7 T in this case) spectrometers and data processing (Fig. 2). Fig. 5 suggests that the nominally 55.6% Na_2O glass of that study [36] probably was about 1% lower in actual alkali content. The nominal 50% Na_2O glass from a more recent study [23] clearly has a quite different overall line shape with lower Q^1 and higher Q^3 peak heights (Fig. 2). The Q^1/Q^2 peak height ratio gives an estimated true Na_2O content of about 47.3 ± 0.5% (Fig. 5). The NMR spectrum for the nominally 55% Na_2O glass mentioned in the latter study was not shown and thus this kind of comparison cannot be applied.

^{29}Si spectra for the glasses on nominal 50% K_2O (Fig. 4) show two partially resolved components separated by 4 to 5 ppm, with low 'shoulders' to higher and lower frequencies. In an extensive study of a wide compositional range of K-, Rb-, and Cs-silicate glasses (compositions analyzed by X-ray fluorescence), variations in peak size and position with composition lead to an assignment of these two main components to two distinct populations of Q^2 species, labeled here as Q^2a and Q^2b, with less resolved shoulders corresponding to Q^1 and Q^3 species [35], as in earlier work [36]. In these previous studies, the relative height of the Q^2a (higher frequency) peak increased systematically with higher K_2O content. The shape of the spectrum for our K50–1300 glass is between those for the glasses with 46.7 and 50.0%

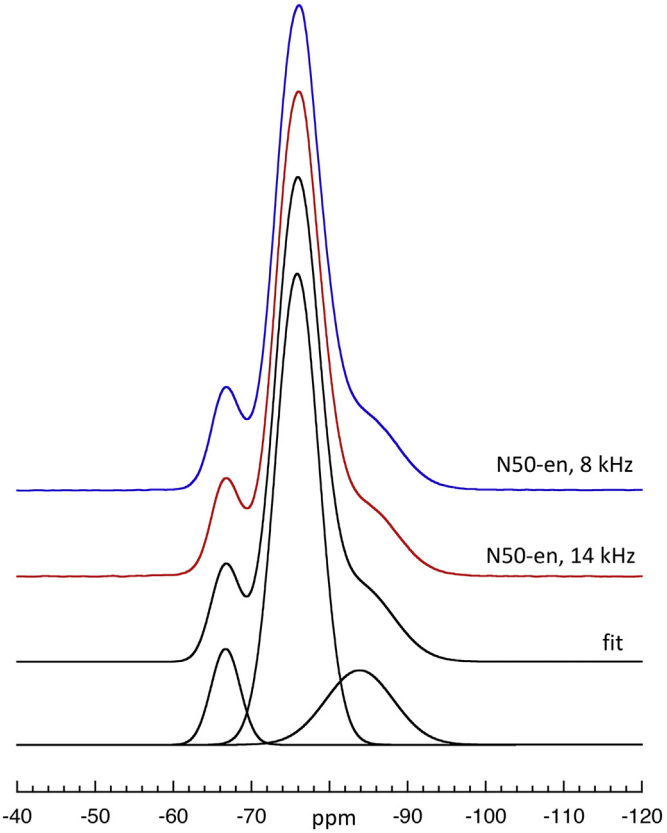

Fig. 3. ^{29}Si MAS NMR spectra of the isotopically enriched (N50-en) sodium silicate glass with close to 50 mol% Na_2O, as in Fig. 2, but with the three-peak fit as described in the text. Also compared are spectra collected with the usual 14 kHz sample spinning rate and a slower 8 kHz rate.

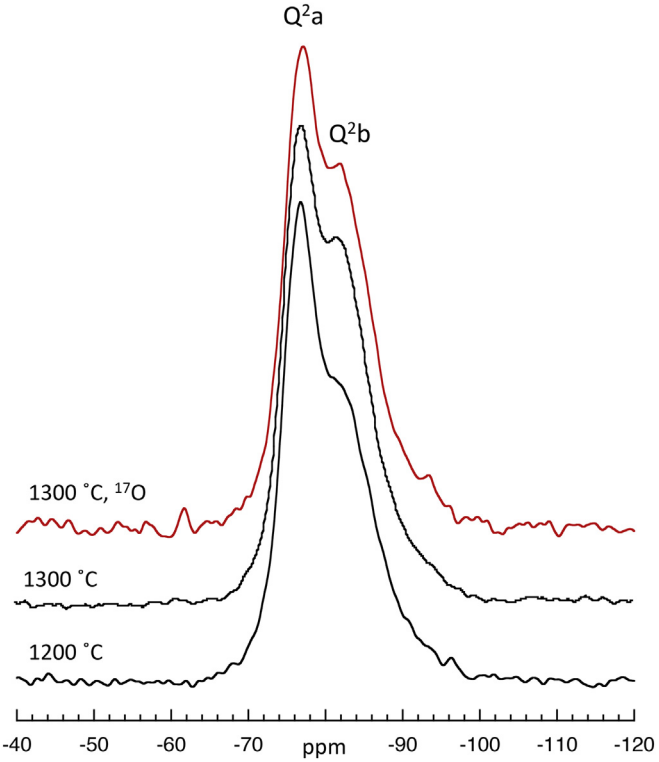

Fig. 4. ^{29}Si MAS NMR spectra of potassium silicate glasses with close to 50 mol % K_2O (see Table 1 for analyzed composition), melted at temperatures shown. The uppermost spectrum is for the ^{17}O-enriched glass. The latter was not analyzed chemically, but its spectrum is nearly identical to the unenriched glass melted at the same temperature. Peak assignments are as in [35].

K_2O in [35], consistent with its analyzed composition of 47.3 ± 0.5% K_2O. The ^{29}Si spectrum for our K50−^{17}O glass (also melted at 1300 °C) is nearly identical, indicating a very similar composition. The spectrum of the K50–1200 glass has a considerably higher Q^2a peak, suggesting significant alkali loss at the higher melting temperature and associated with observed loss of the carbonate signal in the ^{17}O spectra (see below).

For two of the Na-silicate compositions, Table 1 compares data for glasses melted at 1200 °C vs. 1300 °C. For both the N50 and N55 compositions, small decreases in the Q^1/Q^2 peak height ratio for the higher temperature glass can be seen that are consistent with very minor additional alkali loss, but these changes were apparently too small to show up within the precision of the chemical analysis (± 0.5%).

3.2. Effects of sample spinning rate

NMR spectra collected at different magnetic fields and/or sample spinning rates can potentially yield somewhat different results. We have thus tested the latter here. In MAS spectra of spin-1/2 nuclides such as ^{29}Si, if the sample spinning frequency (in Hz) is significantly lower than the frequency span of the static (non-spinning) line shape, some of the overall signal intensity will be transferred to spinning sidebands [37,38]. The width of the static spectrum is characterized by the chemical shift anisotropy (CSA). If the CSA is markedly different for different components (e.g. Q^n species) of a spectrum, their relative contributions to the central line shapes will vary with spinning rate. At a given frequency of observation (proportional to the external magnetic field and the gyromagnetic ratio of the nuclide of interest), more rapid spinning reduces the total intensity of the sidebands and yields a more accurate central line shape. Full accuracy can in principle by obtained by observing and analyzing line shapes of sidebands as well as central peaks [27,39], but readily obtainable signal to noise ratios often mean that central peaks only are considered. Because the absolute frequency (in Hz) of the CSA, like the chemical shift itself, is directly proportional to the external magnetic field, it is constant in ppm units (relative frequency). Thus, scaling the field up by a given factor will require a scaling up of the spinning rate by the same factor to yield a comparable spacing on sidebands in ppm and a comparable spectrum. For example, previously published spectra of Na-silicate glasses near to the 50% composition were collected at a field of 4.7 T (39.8 MHz Larmor frequency) and a spinning frequency of 3.5–4.0 kHz [36] and at 9.4 T (79.4 MHz) and a spinning frequency of 6.0 kHz [23]. These correspond to 10.5 to 12.0 kHz, and 9.0 kHz respectively, at the field employed here (14.1 T, 119.1 MHz), somewhat slower than the 14 kHz used for most spectra shown here.

The high signal-to-noise ratios for spectra obtained here on ^{29}Si-enriched N50-en glass allow effects of spinning rate to be evaluated and thus more meaningful comparison of our results with literature data for this critical composition. Detailed comparison of spectra on this glass from 8.0 vs. 14.0 kHz showed only small differences in the central line shapes that would probably go undetected in data for isotopically normal glasses (Fig. 3). Total observable sideband intensity ranged from about 16 to 7% from the lower to higher spinning rate. Central Q^1 and Q^3 peaks for slower spinning were both very slightly higher. Fitting of such spectra with and without the first two pairs of sidebands produced differences in species abundances that were, however, less than 0.2%. Thus, the CSA's for these three species are similar and, within this range of fields/spinning rates, spectra should be comparable. Some CSA data for alkali silicate glasses supports this observation [8,9,39]. It is important to note, however, that for more symmetrical Q^0 and Q^4 sites, which are known in crystalline silicates to generally have much lower

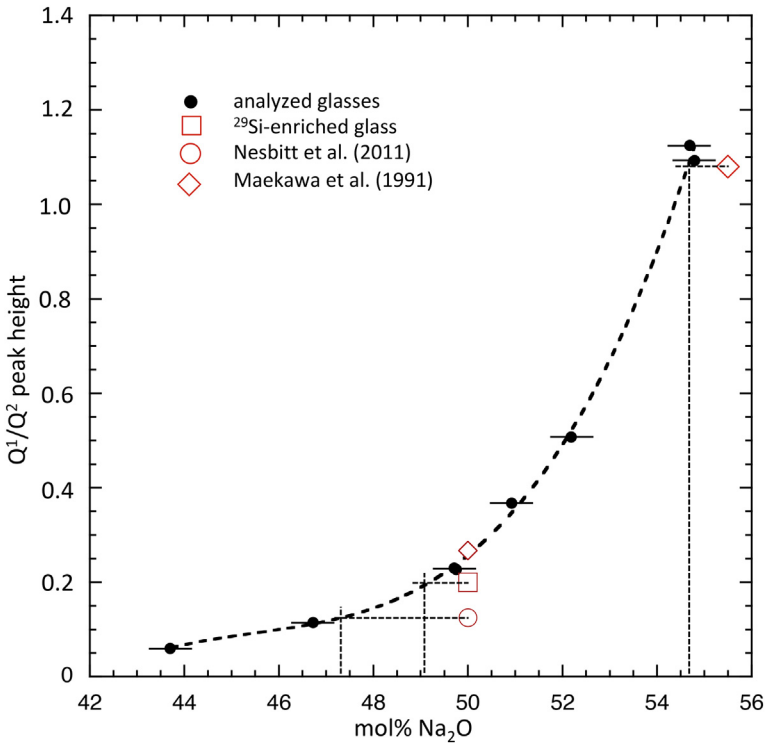

Fig. 5. Plot of ratio of measured peak heights Q^1/Q^2 (not fitted components) vs. analyzed composition for isotopically normal sodium silicate glasses (solid circles with error bars). The long-dashed curve is a polynomial fit for interpolation only. The open square shows the measured Q^1/Q^2 for our ^{29}Si-enriched glass (nominally 50 mol% Na_2O) and indicates that its composition is close to 49.2% Na_2O (short-dashed lines). Similarly, Q^1/Q^2 peak height ratios from two glasses of nominally 50% Na_2O from previous studies indicate in one case significant divergence from the nominal composition (open circle [23]). Data for a glass with nominal 55.6% Na_2O also indicate that its actual Na_2O content is somewhat lower (open diamond [36]).

CSA's than Q^2 and Q^3 groups [37,40], their contributions to central line shapes in glasses may be exaggerated at relatively slow spinning rates, for compositions in which such species are abundant.

3.3. Fitting results for ^{29}Si MAS spectra

Fitting of ^{29}Si MAS NMR spectra has long been used to estimate relative proportions of Q^n species in alkali silicate glasses [4,5,7], although in some special cases (e.g. Q^4 concentrations) "static" (non-spinning) may be more informative [8,9,36]. All such fitting procedures are to some degree model-dependent. Most commonly, symmetrical Gaussian functions, together with least-squares regression, are used to derive component peak areas. In many cases, such fits do yield good approximations to experimental data, e.g. in the special case of pure SiO_2 glass (Q^4 only). Some proportion of Lorentzian line shape is sometimes added during fitting, primarily to account for 'tails' of spectra at unexpectedly high and low frequencies around the central peak. In spectra of solids, these may be caused by very rapid relaxation of some portion of the signal because of proximity of some Si atoms to paramagnetic centers, or, in 'soft' materials, to dynamical effects, or simply to experimental imperfections such as curving baselines. (In simple, low viscosity liquids in contrast, NMR peaks are often inherently Lorentzian because relaxation is controlled by rotational or other dynamics describable by simple exponential functions [41].) There is some justification for Gaussian line shapes in solid-state NMR of spin-1/2 nuclides in glasses (and in other spectroscopies such as Raman and XPS), as simple representations of "random" or "disordered" structure. However, there is often no clear definition of what "random" means in this case. More importantly, it is not always obvious that a "random" variation about a mean, which might be expected for some structural parameter that affects chemical shielding (e.g. first neighbor bond distances or angles), should map linearly into the observed chemical shift. It is thus possible that non-Gaussian line shapes, possibly non-symmetrical in form, could be the best representation of actual component contributions from distributions of individual Q^n species. Any fitting procedure for such more complex line shapes, however, is likely to involve more adjustable parameters and thus be more difficult to accurately constrain from a given, noise-containing data set. In one early study, for example, these issues were explored in some depth for various non-Gaussian and asymmetrical line shapes, fitted to relatively noisy (S/N ca. 20–40) ^{29}Si MAS spectra for several sodium silicate glasses with carefully analyzed compositions, demonstrating the challenges in deducing accurate species proportions from such data [42].

We have partially explored this issue by tests of several fitting assumptions for the spectra of the ^{29}Si-enriched glass N50-en, which typically had S/N of about 1500, at least an order of magnitude greater than that typically attained for isotopically normal samples. Initial fits with one component each for Q^1, Q^2 and Q^3 (with no clear evidence of Q^0 or Q^4 at the > 1% level) and allowing a variable fraction of Gaussian vs. Lorentzian components in the lineshape generally yielded > 95% Gaussian. Therefore, in further fitting, this parameter was fixed at 100% to reduce the number of adjustable parameters. For this sample, we found a significant contribution to the fitting residual to be a slight asymmetry in the main Q^2 peak, skewed slightly to the low frequency (more negative chemical shift) side. This asymmetry was approximated by introducing a second Q^2 component at a 2.5 ppm lower frequency than the main peak (Figs. 2 and 3, Tables 1, 2), which lowered χ^2 by about a factor of 3. Similar 3- and 4-peak fits were made for the spectra of the isotopically unenriched glasses (Table 1) ranging from 44 to 51% Na_2O. For the nominally 55% Na_2O glasses, tests were also made of one vs. two Q^1 peaks to account for a possible asymmetry in this major component. A small contribution from Q^0 species was also seen in the highest-Na compositions and modeled by an additional small Gaussian peak. Representative results from these fitting exercises are shown in Figs. 2 and 3 and in Tables 1 and 2, as well as Fig. 9 (below).

We place no structural significance on such unresolved 'extra' spectral components (e.g. two Q^2 peaks) apart from their potential improvement in modeling the lineshapes for the major species, as these may simply represent one (likely non-unique) way to approximate an asymmetric NMR peak for a continuous range of structural variation (e.g. bond distances or angles). In some cases, for example a combined ^{29}Si and ^{17}O NMR study of high silica potassium silicates two component fits (in that case two Q^4 peaks) can be justified as representing sites

Table 2
Examples of fitted components for ^{29}Si-enriched glass (N50-en, shown in Figs. 2 and 3).

	Center, ppm	FWHM[a], ppm	area, %
4 peak fit (preferred)			
Q^3	−84.7	9.7	15.1
Q^2A	−75.5	6.2	58.7
Q^2B	−78.0	6.7	16.0
Q^1	−66.8	4.5	10.2
3 peak fit			
Q^3	−83.9	10.2	17.8
Q^2	−75.9	6.5	72.4
Q^1	−66.7	4.4	9.9

[a] Full width at half maximum height.

with different next-neighbor populations [43]. In others, partial resolution of peaks, combined with chemical shift systematics and compositional constraints, lead to assignment of two NMR spectral components to the same Q^n species, for example the extensive studies of lower-silica potassium silicates noted above [35,36], which correlates with the lineshape we report here for a single composition in this system (Fig. 4).

3.4. Results from ^{17}O MAS NMR on K-silicate glasses and K_2CO_3

^{17}O NMR results for K-silicate glasses are reported here, as chemical shift separations of different oxygen species are expected to be considerably larger than for comparable Na-silicates [30,44]. The central regions of ^{17}O MAS spectra for the ^{17}O-enriched K50 glasses are shown in Fig. 6. As is well-known from previous work [31,44], K-silicates show two partially overlapping peaks attributable to bridging (BO) and nonbridging (NBO) species. For quadrupolar nuclides such as ^{17}O (nuclear spin $I = 5/2$), quadrupolar coupling typically broadens peaks, shifts them down in frequency, and leads to asymmetrical line shapes. These effects depend strongly on the Larmor frequency (and hence external field) as well as the quadrupolar coupling constant (C_Q) for a given species. In silicates, C_Q values for nonbridging oxygens are known to be generally much smaller than for Si-O-Si bridging oxygens [37,44–46]. At the 14.1 T field used here, ^{17}O MAS NMR peaks for NBO in glasses are roughly Gaussian in form, but BO peaks generally show clear residual quadrupolar line shape effects, e.g. skewing to lower frequency. Given also the complex effects on central peak intensities for non-infinite spinning rates [37,47,48], re-interpretations of such overlapping components in spectra by fitting with Gaussians or even combinations of Gaussians (particularly when sideband intensities are not considered) are likely to yield inaccurate estimations of true species proportions [26]. For the purposes of this study we have not attempted to derive NBO and BO contents from the K50 glass spectra. However, it is clear that initial melting at a higher temperature lead to visible reduction in the proportion of NBO coincident with greater alkali volatilization (Fig. 4).

The spectrum of the glass melted at 1200 °C (Fig. 6) showed an additional small, relatively narrow peak (ca. 20 ppm full width at half maximum height, FWHM) centered at 139 ± 2 ppm, comprising about 0.7% of the central transition NMR signal. This component disappeared completely when the same glass was remelted at 1300 °C. Suspecting that this could be due to carbonate groups, we synthesized ^{17}O-enriched K_2CO_3 as described in the experimental section. Its spectrum consisted of a relatively narrow peak, centered at 134 ppm with a FWHM of 21 ppm. Given that the crystal structure contains 3 inequivalent O sites [49], this is likely to be a composite peak and is not amenable to accurate fitting with a quadrupolar line shape. However, the overall peak width indicates a maximum mean C_Q of about 3.5 MHz and thus an isotropic chemical shift between about 145 and 134 ppm. (These can be compared to values 6.97 MHz and 204 ppm for ^{17}O in $CaCO_3$ [50].

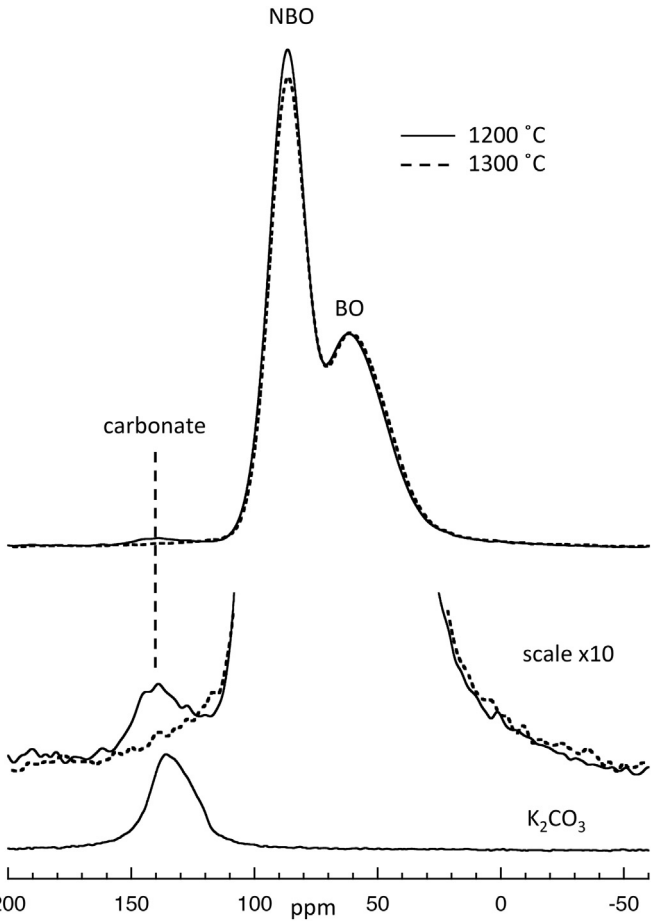

Fig. 6. ^{17}O MAS NMR spectra of ^{17}O-enriched potassium silicate glasses with close to 50 mol% K_2O, melted at temperatures shown (see Table 1 for analyzed composition of K50–1300 °C). Also shown are data for crystalline ^{17}O-K_2CO_3. Non-bridging (NBO) and bridging (BO) oxygen peaks are labeled. The spectra for the glasses are normalized to the BO peak height; the vertical scale for the K_2CO_3 is arbitrary.

Given known effects of cation charge and size on ^{17}O chemical shifts for simple oxides and NBO [37], the difference between K_2CO_3 and $CaCO_3$ may be expected, but the apparently small C_Q for K_2CO_3 seems surprising given the asymmetry in the bonding environment of O in carbonate groups.) The 5 ppm difference in peak position from the comparable feature in the K50 glass spectrum suggests that the carbonate, if actually dissolved in the glass, has a similar but not identical bonding environment compared to that in the crystal (one C and five K first neighbors); alternatively the difference might be due to a particle size or strain effect if the carbonate actually crystallized to a separate phase during quench of the glass. In either case, given that ^{17}O was added to glass as SiO_2, there was considerable isotopic exchange between silicate and carbonate groups.

Fig. 7 shows higher frequency regions of the spectra, where signals from “free” oxide ions (“FO” or O^{2-} anions coordinated only by K^+ cations) are expected from theoretical calculations in the region of about 300 to 400 ppm [31]. Data from two spinning rates are shown to reveal different parts of the baseline between the spinning sidebands. As previously noted for a 40% K_2O silicate glass [31] and in several Ba and Ca-silicates [48], there is no indication of any additional features in this area of the spectra that could be attributed to FO, although data from an even higher field and much faster sample spinning would be helpful.

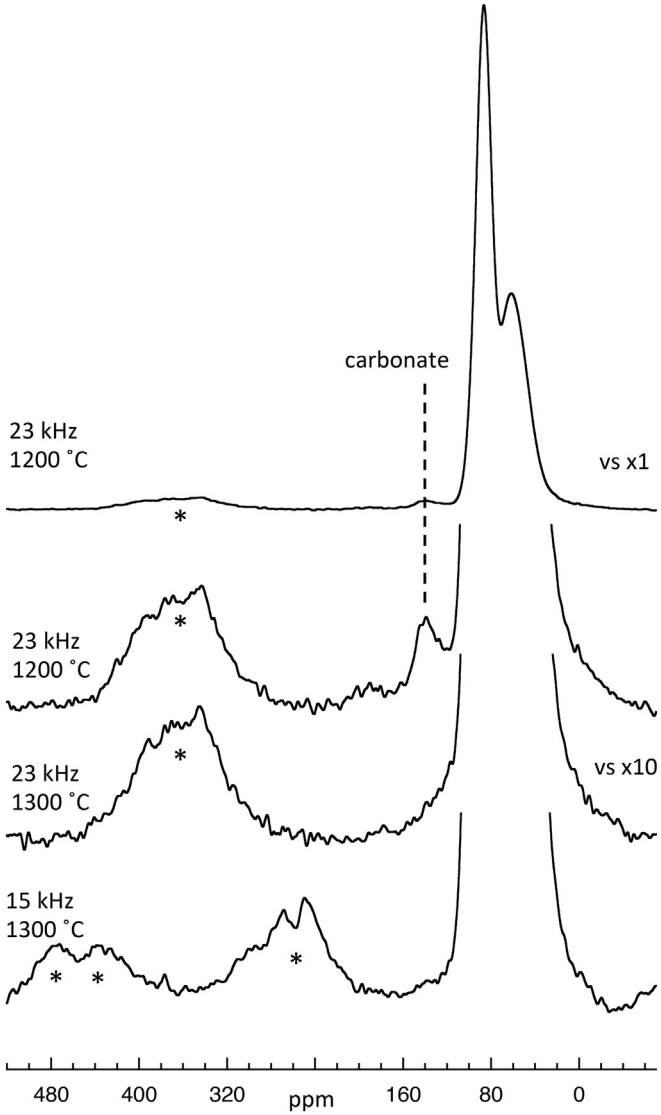

Fig. 7. ^{17}O MAS NMR spectra of ^{17}O-enriched potassium silicate glasses with close to 50 mol% K_2O, melted at temperatures shown, showing a wider frequency range. Data for two different sample spinning rates are shown to better reveal the baseline in region of 300 to 400 ppm. Spinning sidebands are marked by *. In the lower three spectra, the vertical scaling is multiplied by 10× relative to that of the top spectrum. The tiny sharp peak near to 380 ppm is a background signal from the zirconia sample rotor.

3.5. ^{23}Na MAS NMR spectra

Representative ^{23}Na MAS spectra of the Na-silicate glasses, as well as crystalline sodium metasilicate (NMS) starting materials, are shown in Fig. 8. For the NMS reagent, its spherical particles packed into the NMR rotor with random orientations, resulting in a quadrupolar line shape fully consistent with previous data (isotropic chemical shift δ_{iso} of 22.1 ppm when referenced to aqueous NaCl, C_Q = 1.4 MHz, quadrupolar asymmetry parameter η = 0.7 [29,51]). This spectrum also showed the presence of small amounts of at least one other Na-containing phase, consistent with the slight excess of Na/Si in glasses made from it (Table 1). The other primary NMS starting material showed no extraneous phases but a somewhat distorted central peak shape consistent with an orientationally non-random packing of its elongate crystal fragments in the NMR rotor, an issue well-known from previous studies of this phase [29].

As is typical for spectra of glasses, those for the glasses studied here

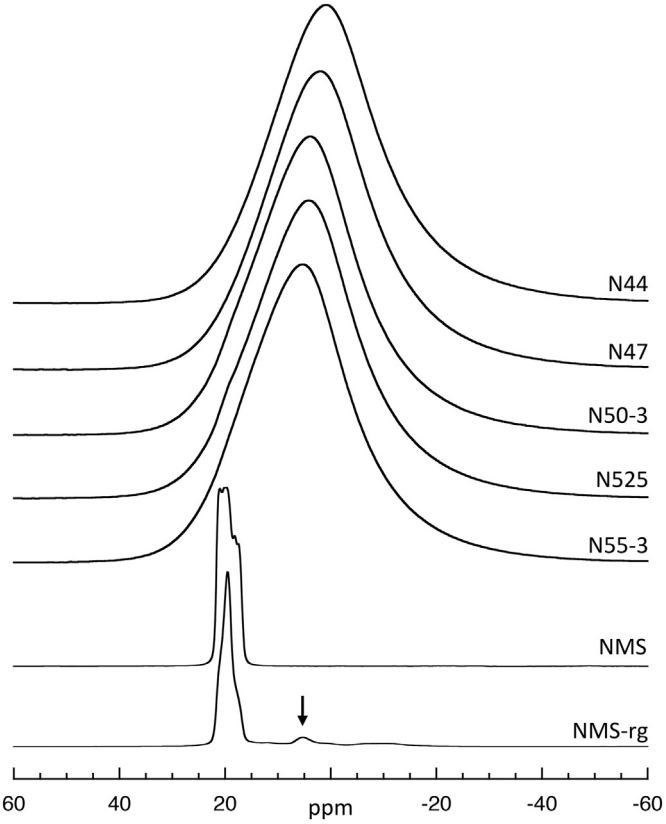

Fig. 8. ^{23}Na MAS NMR spectra of sodium silicate glasses. Also shown are data for the crystalline sodium metasilicate starting materials for the glasses. "NMS" is the isotopically normal sample from a previous study [28] and shows only a single phase; "NMS-rg" is a commercial reagent that contains a slight excess of Na_2O and at least one extra peak in the spectrum, noted by arrow. Spectra for the glasses are normalized to the same maximum intensity; the vertical scales for the spectra of the crystals are arbitrary.

are broad and asymmetrical, with no resolution of signals from Na^+ cations in different bonding environments (Table 3, Fig. 8). Both distributions of chemical shifts (due to structural disorder) and quadrupolar broadening may contribute to such line shapes; the latter also shifts the resonances down in frequency. Data collected at multiple magnetic fields, and/or by multiple-quantum NMR methods, can help to discriminate such contributions [52–54] and indicate that in silicate glasses at 14.1 T, the chemical shift is probably predominant. The latter is in turn highly correlated with mean first-neighbor Na—O bond distance (longer bonds, lower δ_{iso}) and therefore decreases with higher Na coordination numbers [55,56]. Thus, as seen previously in other studies, the slight progression in peak maximum from the highest to lowest Na_2O glass studied here (5.4 to 0.7 ppm) is most likely related to a slight increase in mean coordination number as, on average, more BO and fewer NBO are present in the Na^+ cation first shells. Given that the Na coordination number in crystalline Na_2SiO_3 is five (Na—O ranging from 0.2289 to 0.2455 nm with mean of 0.2370 nm [57]), most of the Na^+ cations probably have coordination numbers of five and higher.

3.6. Constraints on anionic structure near to the Na_2SiO_3 composition

Q^n species abundances, derived from ^{29}Si NMR, Raman, and other spectroscopies have often been used to evaluate models of glass structure for relatively simple compositions, particularly alkali silicate and alkaline earth silicates [1]. Usually implicit in such discussions is that the observed structure represents that of an equilibrium (supercooled) liquid at some temperature. In fact, at best the structure of the glass represents that quenched in at the fictive temperature, the point at

Table 3
Glass compositions, non-bridging oxygen, and "free" oxide contents estimated from ^{29}Si fitting results; ^{23}Na NMR data.

Name	T, °C	%Na_2O meas.[a]	%Na_2O fit 1	%Na_2O fit 2	NBO/Si meas.[b]	NBO/Si fit 1[c]	NBO/Si fit 2[c]	FO fit 1[d]	FO fit 2[d]	^{23}Na max. ppm[e]	^{23}Na FWHM ppm[f]
N50-en	1200	49.2	49.0	49.4	1.94	1.92	1.95	0.2	−0.2		
N50–1	1360	49.8	49.1	49.7	1.98	1.93	1.98	0.9	0.1		
N50–2	1200	49.7	49.2	49.6	1.98	1.94	1.97	0.6	0.1		
N50–3	1200	50.9	50.7	51.0	2.07	2.06	2.08	0.3	−0.2	4.0	22.9
N55–2	1200	54.7	54.3	54.5	2.42	2.38	2.40	0.6	0.3		
N55–3	1300	54.8	54.1	54.5	2.42	2.35	2.40	1.1	0.4	5.4	22.7
N525	1200	52.2	51.6	51.9	2.18	2.13	2.16	0.8	0.4	4.2	22.9
N47	1300	46.7	46.4	46.7	1.75	1.73	1.75	0.4	0.0	2.1	22.9
N44	1300	43.7	43.5	43.7	1.55	1.54	1.55	0.2	0.0	0.7	23.4

[a] mole % measured by titration, except N50-en, which was estimated from NMR peak height data in Fig. 5.
[b] non-bridging oxygens per Si, calculated from composition and assuming negligible FO, labeled as "N_{obs}" in text.
[c] calculated from fitted Q^n components, labeled as "N_{cal}" in text.
[d] calculated from fitted Q^n components and measured composition.
[e] peak maximum.
[f] full width at half maximum height.

which the liquid structure can, because of slowing dynamics, no longer change its configuration to a more ordered state in response to cooling. For a group of glasses quenched at similar rates, the fictive temperatures will be mirrored by the directly-measurable glass transition temperatures, T_g. We did not measure T_g for our samples, but other studies indicate that they are not expected to vary by more than 20 to 30 °C within the narrow compositional range explored here, and will be at roughly 420 °C [35,58]. Q^n species concentrations in liquids are known to be functions of temperature, with reactions such as [1] usually shifting to the right at higher T [16,59,60], but expected variation over the relevant range of fictive temperatures should also be negligible. However, distributions of bridging and non-bridging oxygens are likely to be considerably more disordered at liquidus temperatures of interest in thermodynamic models of phase equilibria, physical properties, etc., resulting in a wider range of Q^n species.

As in previous studies [4,7,35,36], we begin by modeling the simplest single equilibrium that will control most of the Q^n speciation over this compositional range, ignoring possible small concentrations of other species:

$$2Q^2 \Longleftrightarrow Q^3 + Q^1 \quad (3)$$

The balance among these species is often treated as an "apparent" equilibrium constant (ignoring any changes in activity coefficients with composition) for this reaction (or for others involving Q^4 and Q^0 species), labeled here as K_2. Fig. 9 shows calculated Q^1, Q^2, and Q^3 species for such a model, constrained by approximate estimated concentrations at the 50% composition (Q^1 = Q^3 = 13%, Q^2 = 74% of total). The agreement with our measured values is good, probably within error given compositional uncertainty and variations in outcomes of different fitting assumptions. Q^1 contents at the highest sodium contents may be over-predicted because of neglect of the non-negligible Q^0 content in this simple model; fitted values of Q^3 contents in these compositions may in turn be overestimated given the uncertainty in fitting such a low, broad shoulder. The corresponding K_2 value for this model is 0.0309, but its precision is relatively low. For example, variation in the constraints at the 50% composition of ± 2% absolute in Q^2 (i.e. from 72 to 76% of total) move the ends of the model curves on Fig. 9 (i.e. Q^2 concentrations at 44 and 55% Na_2O) by less than ± 0.5%; corresponding estimates of K_2 would be 0.038 and 0.025.

Also shown in Fig. 9 are several Q^n species concentrations reported in two earlier NMR studies of glasses in this range [23,36], plotted both at their nominal and their corrected mole % Na_2O as described above, using the Q^1/Q^2 peak height ratio (and thus independent of any fitting model). Agreement is good among such data sets once this adjustment has been made. Note that it is not recommended to extend this correction procedure outside of the range shown, as it will be most effective only when these two peaks are relatively intense and well-resolved.

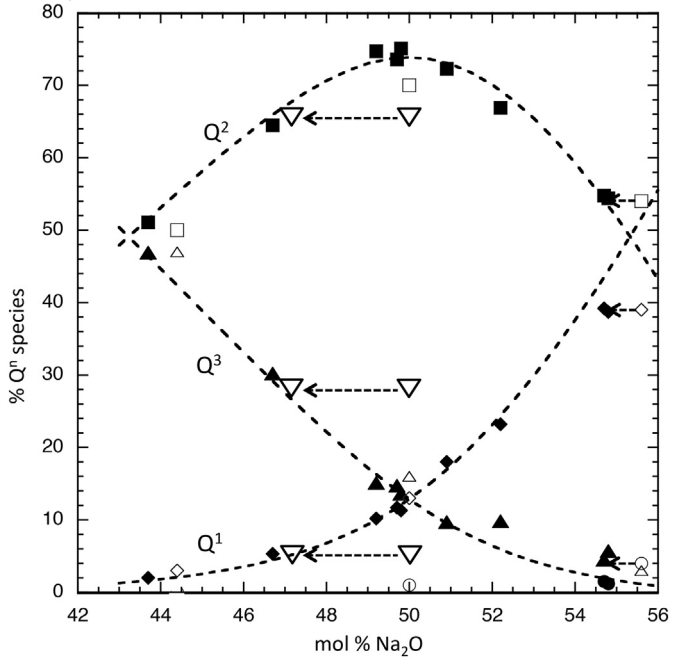

Fig. 9. Q^n species derived from fitting ^{29}Si NMR spectra vs. those predicted by a simple model accounting only for Q^1, Q^2, and Q^3 groups (see text). Solid symbols are new data, with squares for Q 2, triangles for Q^3, diamonds for Q^1, and circles for Q^0 (55% Na_2O only), plotted at analyzed compositions. Open symbols are from previous studies by others, plotted at published nominal composition and adjusted in composition (dashed arrows) when feasible based on measured Q^1/Q^2 peak heights (independent of fits, as in Fig. 5). Inverted triangles from [23]), others from [36].

A common test of consistency of such models is to sum the NBO per Si (NBO/Si or N_{obs}) directly from the observed Q^n species proportions (as fractions totaling 1), with:

$$N_{obs} = 4 \times Q^0 + 3 \times Q^1 + 2 \times Q^2 + 1 \times Q^3 + 0 \times Q^4 \quad (4)$$

If no other anionic species are present, N_{obs} should agree within uncertainties (including those in composition) with N_{cal}, the value

calculated from stoichiometry (here, simply the mole fraction of Na_2O):

$$N_{cal} = 2\,X_{Na2O}/(1–X_{Na2O}) \quad (5)$$

Table 3 shows results for the glasses studied here. For the simplest fitting exercise (one Gaussian component for each Q^n species), N_{obs} is slightly (about 1 to 2.5%) lower than N_{cal}. For the fits which simulate asymmetry of the largest peaks by adding a second Gaussian component (especially for the Q^2 peak), agreement is within about 1% for all compositions and the difference may be either positive or negative. An estimated uncertainty of 0.5% (absolute) or 1% (relative) in the analyzed percentage of Na_2O near to the 50% composition (i.e. a range of true compositions of 50.5 to 49.5%) propagates to ± 2% in N_{cal} (i.e. a range in N_{cal} from 1.96 to 2.04) Including likely uncertainties in fitting models as well, we consider this comparison to indicate that such a simple model is indeed a good approximation of the structure. Another assumption inherent in this analysis is that Si cations with higher coordination numbers (e.g. SiO_5 groups) are neglible. Pentacoordinate Si has indeed been detected at up to 0.3% by NMR in much higher silica content glasses formed at ambient pressure, but decreases to undetectability above about 25% K_2O [61]. The concentration of SiO_5 groups in alkali silicates reaches the per cent level only at pressures greater than 1 to 2 GPa [62].

Systematic discrepancies between N_{obs} and N_{cal} in this sort of analysis could, in principle, be due to systematic errors in composition and/or to the fitting model used to derive the Q^n species, e.g. the peak asymmetry explored here. It has long been recognized that systematic observation of a value of N_{obs} below that of N_{cal} could also be the result of an incomplete accounting for anionic species; in contrast a value of N_{obs} greater than that of N_{cal} cannot be explained in this fashion [36,63,64]. Most interesting is perhaps the possibility that the reaction of the modifier oxide added to silica to form non-bridging oxygens does not go to completion, an approximation assumed for eq. [5] above. Reaction [2] can be characterized by an “apparent” equilibrium constant (again, ignoring activity coefficients) based on the mole fractions of the three oxygen species:

$$K_{ox} = NBO^2/(FO \times BO) \quad (6)$$

In conventional models of glass-forming silicates with mole fractions of silica far above the orthosilicate stoichiometry (i.e. $SiO_2 > > 33.3\%$), the FO concentration is assumed to be negligible, at least for the purpose of counting Q^n species. K_{ox} is thus treated as effectively infinite, but in practice, with real limits on experimental detection, this means K_{ox} is taken as greater than roughly 100 to 200 [65]. Small but non-zero concentrations of FO may, of course, be significant to models of thermodynamic activities of modifier oxide components (as has long been considered in models of low-silica metallurgical slags [21,22,66,67], as well as to dynamical processes in liquids such as bond-breaking during diffusion and flow [68].

Such an excess in FO, cast as a percentage of total oxygen, can be readily calculated from NBO/Si derived from Q^n speciation (N_{obs}) and X_{Na2O}, with:

$$FO = 100[X_{Na2O}–0.5N_{obs}\,(1–X_{Na2O})]/(2–X_{Na2O}) \quad (7)$$

Values derived from the two fitting schemes described here are shown in Table 3. For the simple Gaussian model (fit 1), FO values are all slightly positive (as dictated by the N_{obs} systematics mentioned above) but with one exception are below 1% of total oxygen; for the model simulating asymmetric Q^2 peaks (fit 2) the FO values are close to zero and may be slightly positive or negative. A maximum value of FO at the 55% Na_2O composition of 0.5 to 1% would predict minimum values of K_{ox} of 455 to 217; a maximum value of FO of 0.5% at the near 50% composition (better constrained by the high signal-to-noise data for the isotopically enriched glass) would predict a minimum value of K_{ox} of 255. Much larger values of K_{ox} would of course be consistent with even lower FO values and thus with these data, but are simply not well constrained by these measurements. Such values have, for example, been suggested by the extremely negative free energies of formation of crystalline alkali silicates in comparison with those of alkaline earth and transition metal silicates [65]. It is also important for discussions of liquid (as opposed to glass) properties, including solid-liquid-vapor phase equilibria, that the likely exothermic nature of reaction [2] in all alkali and alkaline earth systems predicts increase significantly FO content with increasing temperature [65]. In any case, the data and analysis presented here suggest that K_{ox} at typical fictive temperatures for alkali silicates (ca. 400–500 °C) is most likely to be much greater than estimated values as low as 2 (ca. 14% FO at X = 50%) [25] to 8 (ca. 8% FO at X = 50%) [24] derived from fitting oxygen 1 s XPS spectra for K-silicate glasses, to 14 (ca. 5% FO at X = 50%) derived from XPS of Na-silicates [23]. The latter was considered to be consistent with accompanying ^{29}Si NMR data, but as noted above (Figs. 2 and 5) the published NMR spectrum for the critical (nominal) 50% Na_2O glass is more consistent with a true composition with 2–3% lower alkali content.

Many previous studies of NMR and other spectra of alkali silicate glasses have made such comparisons. In an extensive study of much wider compositional ranges of Li-, Na- and K-silicates [36], for example, it was concluded that values of NBO/Si derived from fits to spectra (N_{obs}) agreed within error of those predicted from nominal compositions (N_{cal}) for the Na_2O and K_2O binaries but that in the Li_2O system significant FO might be present. However, nominal glass compositions were used. In a more recent study of K-, Rb- and Cs-silicates, also over wide compositional ranges, glass compositions were carefully analyzed by X-ray fluorescence [35]. When deriving Q^n speciation from simple Gaussian fits, the authors noted a slight deficiency in N_{obs} vs. N_{cal} but found that this could be eliminated (without important effects on quality of fit) by constraining relative peak areas during fitting. (Similar constraints have often been used in deriving Q^n speciation from Raman spectra [1]). As noted above, modeling of those data for K-silicates was complicated by the appearance of a second partially resolved feature in the spectra most obviously attributable to Q^2 groups with a distinct range of chemical shifts; this makes testing (as done here for Na-silicates) of peak asymmetries less practical. A re-interpretation of those results, assigning one of the assumed Q^2 components to a second type of Q^3 group, produced a much greater NBO/Si deficit and thus much higher calculated FO content more similar to those estimated from XPS data [24], but this was considered to be inconsistent with known chemical shift systematics [69,70].

Perhaps the most stringent available ^{29}Si NMR-Q^n speciation test for abundant excess FO in alkali silicate glasses is a study of Li-silicate glasses prepared by roller quenching (cooling rate ca. 10^5 K/s) out to 64 mol% Li_2O [27]. For example, a value of K_{ox} of 14, as deduced for Na-silicates from XPS spectra [23], would predict an FO content of about 15% of total oxygen at this composition. However, the authors showed good agreement between NBO/Si derived from fitted Q^n speciation (presented as the calculated Li_2O content) to that predicted from nominal compositions, using the conventional assumption of negligible FO. If a rough guess is made about maximum excess FO allowed by uncertainties in either fits or compositions in that study of 1 to 2%, the estimated minimum K_{ox} value would be 1380 to 570. The higher cation field strength (charge divided by square of the mean cation-oxygen distance [71]) of Li^+ relative to Na^+ and K^+ should also enhance FO content, based on well-known effects of field strength on oxide ion activities of low-silica metallurgical slags in which this species must be abundant, as well as through effects of systematics of reaction energies between modifier oxides and silica [65]. K_{ox} values in Na- and K-silicates might thus be expected to be even higher than in Li-silicates.

All of the estimates of free oxide concentration described so far are indirect, in that they involve fitting and interpretation of spectra for other species, such as Q^n species in ^{29}Si NMR spectra or BO and NBO in oxygen 1 s XPS data or ^{17}O NMR. Direct observations of free oxide species would be obviously helpful in better refining models of anionic speciation in silicate glasses and melts. So far, the most convincing

results of this type have been ^{17}O MAS studies of Pb silicates [72], where NMR signals for significant concentrations of FO were clearly resolved even for compositions where this species is not required by stoichiometry (SiO_2 > 33%) (qualitatively consistent with previous oxygen 1 s XPS data showing the clear presence of non-stoichiometric BO contents in a Pb-orthosilicate glass [20]). Oxygen sites coordinated only by Hf^{4+} cations were also clearly seen in sputter-deposited thin films of HfO_2-SiO_2 that may mimic the behavior of deeply supercooled liquids [73]. Both of these systems are, however, chemically quite different from alkali silicates in their greater strength of interaction of the modifier cation with the oxide ion. Somewhat closer in behavior are mixed Ca−Mg silicate glasses, which can be made by rapid-quench methods to as low as about 33 to 28% SiO_2 [74]. Here, up to about 10% FO (probably bonded to Mg^{2+}) were directly observed, albeit with a relatively complex, two-dimensional, double resonance NMR experiment [75]. The cation field strength of Mg^{2+} is of course much higher than those of the alkali cations, probably promoting the formation of FO.

Because chemical shift separations among oxygen species in one-dimensional ^{17}O MAS NMR spectra are known to increase with the size of the modifier cation, studies of Ca- and K-silicate may be more revealing than those of Mg- and Na-silicates. As described above, no signal for FO was detected in a previous study of a ca. 40% K_2O silicate glass, and here for a composition (K50) with about 47% K_2O. It is of course difficult to assess a detection limit for a negative finding of this type, as expected chemical shift and quadrupolar broadening are not well-known. However, ^{17}O NMR signals from relatively distorted FO sites in crystalline Ca_3SiO_5 are quite narrow and readily resolved by simple MAS NMR [48]. Those in the high pressure wadsleyite polymorph of Mg_2SiO_4 were readily seen using ^{17}O using multiple-quantum or ultra-high field NMR to avoid chemical shift overlaps [76,77]. If an FO NMR peak in the K50 glass described here were as narrow as that observed for the carbonate groups, it could be detected below the 0.5% level; if an FO peak were instead much broader, e.g. comparable to the spinning side bands, it could probably be detected at the roughly 2% level. These are well below the FO content of about 6 to 7% predicted by a model of K-silicates based on fits of oxygen 1 s XPS spectra (K_{ox} = 8 [24]). Scenarios can be imagined in which an as-yet unobserved feature in a glass spectrum could be even broader and more difficult to detect, for example a high degree of local disorder and hence a wide range of chemical shifts, but given the likely strong ionic interactions between an O^{2-} ion and modifier cations, the local environments of FO groups would be expected to be relatively ordered.

4. Conclusions

The data presented here for ^{29}Si MAS NMR spectra of Na silicate glasses in a narrow range around the critical 50% silica content show marked, compositional-dependent changes in heights of resolved peaks attributable to Q^1 and to Q^2 species, independent of fitting models. Together with accurate and precise chemical analyses, these can be used to compare new results with those previously published in this range, and can bring these into consistency. In some cases, true alkali contents may be considerably lower than nominal. Simple fits (one component for each species) with Gaussian line shapes of the relatively noisy spectra obtainable with standard starting materials may lead to estimated NBO/Si ratios that are slightly lower than those expected from stoichiometry, given conventional assumptions that all oxygens are coordinated by one or two Si cations, as has been noted in other studies [23,35]. A small percentage (ca. 1%) of unreacted “free oxide” could be postulated to explain this discrepancy, although this value would be considerably lower than other recent estimates for this composition based primarily on XPS data [23]. However, much higher quality NMR spectra obtainable for a glass near to the 50% composition, using ^{29}Si-enriched starting material, indicates that at least the major Q^2 peak is probably slightly asymmetrical, and is more accurately simulated by including a small, second Gaussian component at slightly lower frequency. Such fits of data for the other glasses yield NBO/Si ratios within uncertainty of those predicted from stoichiometry, with concentrations of FO that are below measurable limits. Fits of such spectra with other assumptions or constraints could lead to somewhat different results, but should be justified by clear experimental evidence or more advanced theoretical considerations, such as direct calculation of NMR parameters from structural models [78]. ^{23}Na spectra of these glasses are as unresolved as those of previous studies, and do not indicate any obvious change in speciation of alkali sites apart from a small, progressive shift in coordination as NBO/BO changes with composition. As seen previously for a more silica-rich K-silicate glass [31] (as well as for a lower silica Ca-silicate glass [48]), ^{17}O MAS NMR reveals no direct evidence for any FO species, although results could be improved by data from higher magnetic fields and much faster sample spinning rates. Smaller concentrations of FO could be still be of potential interest to models of thermodynamic activities and melt dynamics [23], if these could be accurately constrained by direct structural determinations. Higher, and potentially directly detectable, concentrations of FO may perhaps be found in low silica glasses with higher field strength modifier cations, for example technologically important rare earths and transition metals, but such magnetic ions may pose special challenges for NMR spectroscopy.

Credit author statement

J.F. Stebbins is the sole author of this paper. He conceptualized the study, synthesized the samples, did all of the chemical and spectroscopic data collection, analysis and model calculations. He wrote the entire paper.

Declaration of Competing Interest

The authors declare that they have no known competing financial interests or personal relationships that could have appeared to influence the work reported in this paper.

Acknowledgments

This research was supported by the U.S. National Science Foundation, grant numbers EAR-1521055 and DMR-1505185.

References

[1] B.O. Mysen, P. Richet, Silicate Glasses and Melts, Elsevier, Amsterdam, 2019.
[2] J.F. Stebbins, I. Farnan, X. Xue, The structure and dynamics of alkali silicate liquids: a view from NMR spectroscopy, Chem. Geol. 96 (1992) 371.
[3] A.-R. Grimmer, M. Mägi, M. Hähnert, H. Stade, A. Samosen, W. Wieker, E. Lippmaa, High-resolution solid-state ^{29}Si nuclear magnetic resonance spectroscopic studies of binary alkali silicate glasses, Phys. Chem. Glasses 25 (1984) 105.
[4] C.M. Schramm, B.H.W.S. de Jong, V.E. Parziale, ^{29}Si Magic angle spinning NMR study on local silicon environments in amorphous and crystalline lithium silicates, J. Am. Chem. Soc. 106 (1984).
[5] R. Dupree, D. Holland, P.W. McMillan, R.F. Pettifer, The structure of soda-silica glasses: a MAS NMR study, J. Non-Cryst. Solids 68 (1984) 399.
[6] R. Dupree, D. Holland, D.S. Williams, The structure of binary alkali silicate glasses, J. Non-Cryst. Solids 81 (1986) 185.
[7] J.B. Murdoch, J.F. Stebbins, I.S.E. Carmichael, High-resolution ^{29}Si NMR study of silicate and aluminosilicate glasses: the effect of network-modifying cations, Am. Mineral. 70 (1985) 332.
[8] J.F. Stebbins, Identification of multiple structural species in silicate glasses by ^{29}Si NMR, Nature 330 (1987) 465.
[9] J.F. Emerson, P.E. Stallworth, P.J. Bray, High-field ^{29}Si NMR studies of alkali silicate glasses, J. Non-Cryst. Solids 113 (1989) 253.
[10] R.J. Kirkpatrick, T. Dunn, S. Schramm, K.A. Smith, R. Oestrike, G. Turner, G.E. Walrafen, A.G. Revesz (Eds.), Structure and Bonding in Noncrystalline Solids, Plenum Press, New York, 1986, p. 302.
[11] S.A. Brawer, W.B. White, Raman spectroscopic investigation of the structure of silicate glasses. I. The binary alkali silicates, J. Chem. Phys. 63 (1975) 2421.
[12] T. Furukawa, K.E. Fox, W.B. White, Raman spectroscopic investigation of the structure of silicate glasses. III. Raman intensities and structural units in sodium silicate glasses, J. Chem. Phys. 75 (1981) 3226.

[13] D.W. Matson, S.K. Sharma, J.A. Philpotts, Structure of high-silica alkali silicate glasses. A Raman spectroscopic investigation, J. Non-Cryst. Solids 58 (1983) 323.
[14] D. Virgo, B.O. Mysen, I. Kushiro, Anionic constitution of 1-atmosphere silicate melts: implications of the structure of igneous melts, Science 208 (1980) 1371.
[15] B.O. Mysen, D. Virgo, F.A. Seifert, The structure of silicate melts: implications for chemical and physical properties of natural magma, Rev. Geophys. Space Phys. 20 (1982) 353.
[16] B.O. Mysen, J.D. Frantz, Raman spectroscopy of silicate melts at magmatic temperatures: Na_2O-SiO_2, K_2O-SiO_2 and Li_2O-SiO_2 binary compositions in the temperature range 25-1475°C, Chem. Geol. 96 (1992) 321.
[17] H.W. Nesbitt, C. O'Shaughnessy, G.S. Henderson, G.M. Bancroft, D. Neuville, Factors affecting line shapes and intensities of Q^3 and Q^4 Raman bands of Cs silicate glasses, Chem. Geol. 505 (2019) 1.
[18] H.W. Nesbitt, G.M. Bancroft, G.S. Henderson, D.R. Neuville, R.T. Downs (Eds.), Spectroscopic Methods in Mineralogy and Materials Sciences, Mineralogical Society of America, Chantilly, VA, 2014, p. 271.
[19] J.F. Stebbins, X. Xue, G.S. Henderson, D. Neuville, R.T. Downs (Eds.), Spectroscopic Methods in Mineralogy and Materials Sciences, Min. Soc. Am., Chantilly, VA, 2014, p. 605.
[20] K.N. Dalby, H.W. Nesbitt, V.P. Zakaznova-Herzog, P.L. King, Resolution of bridging oxygen signals from O 1s spectra of silicate glasses using XPS: implications for O and Si speciation, Geochim. Cosmochim. Acta 71 (2007) 4297.
[21] C.R. Masson, Anionic constitution of glass-forming melts, J. Non-Cryst. Solids 25 (1977) 3.
[22] P.C. Hess, Polymer model of silicate melts, Geochim. Cosmochim. Acta 35 (1971) 289.
[23] H.W. Nesbitt, G.M. Bancroft, G.S. Henderson, R. Ho, K.N. Dalby, Y. Huang, Z. Yan, Bridging, non-bridging and free (O^{2-}) oxygen in Na_2O-SiO_2 glasses: an X-ray photoelectron spectroscopic (XPS) and nuclear magnetic resonance (NMR) study, J. Non-Cryst. Solids 357 (2011) 170.
[24] R. Sawyer, H.W. Nesbitt, G.M. Bancroft, Y. Thibault, R.A. Secco, Spectroscopic studies of oxygen speciation in potassium silicate glasses and melts, Can. J. Chem. 93 (2015) 60.
[25] R. Sawyer, H.W. Nesbitt, R.A. Secco, High resolution X-ray photoelectron spectroscopy (XPS) study of K_2O-SiO_2 glasses: evidence for three types of O and at least two types of Si, J. Non-Cryst. Solids 358 (2012) 290.
[26] H.W. Nesbitt, G.S. Henderson, G.M. Bancroft, R. Sawyer, R.A. Secco, Bridging oxygen speciation and free oxygen (O^{2-}) in K-silicate glasses: implications for spectroscopic studies and glass structure, Chem. Geol. 461 (2017) 13.
[27] C. Larson, J. Doerr, M. Affitagato, S. Feller, D. Holland, M.E. Smith, A ^{29}Si MAS NMR study of silicate glasses with a high lithium content, J. Phys. Condens. Matter 18 (2006) 11323.
[28] A.M. George, P. Richet, J.F. Stebbins, Cation dynamics and premelting in lithium metasilicate (Li_2SiO_3) and sodium metasilicate (Na_2SiO_3): a high-temperature NMR study, Am. Mineral. 83 (1998) 1277.
[29] T.M. Clark, P.J. Grandinetti, P. Florian, J.F. Stebbins, An ^{17}O investigation of crystalline sodium metasilicate: implications for the determination of local structure in alkali silicates, J. Phys. Chem. B 105 (2001) 12257.
[30] P. Florian, K.E. Vermillion, P.J. Grandinetti, I. Farnan, J.F. Stebbins, Cation distribution in mixed alkali disilicate glasses, J. Am. Chem. Soc. 118 (1996) 3493.
[31] J.F. Stebbins, S. Sen, Oxide ion speciation in potassium silicate glasses: new limits from ^{17}O NMR, J. Non-Cryst. Solids 368 (2013) 17.
[32] TAPPI, Analysis of Sodium Silicate, Test Method T-632 cm-11, Technical Association of the Pulp and Paper Industry (TAPPI) Technical Methods, 2011.
[33] W.F. Scott, Standard Methods of Chemical Analysis, 5th edition, Van Nostrand, Inc., New York, 1939.
[34] E. Bourgue, P. Richet, The effects of dissolved CO_2 on the density and viscosity of silicate melts: a preliminary study, Earth Planet. Sci. Lett. 193 (2001) 57.
[35] W.J. Malfait, W.E. Halter, Y. Morizet, B.H. Meier, R. Verel, Structural control on bulk melt properties: single and double quantum ^{29}Si NMR spectroscopy on alkali-silicate glasses, Geochim. Cosmochim. Acta 71 (2007) 6002.
[36] H. Maekawa, T. Maekawa, K. Kawamura, T. Yokokawa, The structural groups of alkali silicate glasses determined from ^{29}Si MAS-NMR, J. Non-Cryst. Solids 127 (1991) 53.
[37] K.J.D. MacKenzie, M.E. Smith, Multinuclear Solid-State NMR of Inorganic Materials, Pergamon, New York, 2002.
[38] M.J. Duer, Introduction to Solid-State NMR Spectroscopy, Blackwell, Oxford, U.K., 2004.
[39] E. Schneider, J.F. Stebbins, A. Pines, Speciation and local structure in alkali and alkaline earth silicate glasses: constraints from ^{29}Si NMR spectroscopy, J. Non-Cryst. Solids 89 (1987) 371.
[40] K.A. Smith, R.J. Kirkpatrick, E. Oldfield, D.M. Henderson, High-resolution silicon-29 nuclear magnetic resonance spectroscopic study of rock-forming silicates, Am. Mineral. 68 (1983) 1206.
[41] R.K. Harris, Nuclear Magnetic Resonance Spectroscopy, Pitman, London, 1983.
[42] A. Sebald, B. Blümich (Ed.), Solid-State NMR II: Inorganic Matter, Springer-Verlag, Berlin, 1994, p. 91.
[43] S. Sen, R.E. Youngman, NMR study of Q-speciation and connectivity in K_2O-SiO_2 glasses with high silica content, J. Non-Cryst. Solids 331 (2003) 100.
[44] X. Xue, J.F. Stebbins, M. Kanzaki, Correlations between O-17 NMR parameters and local structure around oxygen in high-pressure silicates and the structure of silicate melts at high pressure, Am. Mineral. 79 (1994) 31.
[45] S. Schramm, E. Oldfield, High resolution solid-state NMR studies of quadrupolar nuclei: quadrupolar-induced shifts in variable-angle sample-spinning of a borosilicate glass, J. Chem. Soc. Chem. Commun. (1982) 980.
[46] K.T. Mueller, Y. Wu, B.F. Chmelka, J. Stebbins, A. Pines, High-resolution oxygen-17 NMR of solid silicates, J. Am. Chem. Soc. 113 (1990) 32.
[47] D. Massiot, C. Bessada, J.P. Coutures, F. Taulelle, A quantitative study of ^{27}Al MAS NMR in crystalline YAG, J. Magn. Reson. 90 (1990) 231.
[48] L.M. Thompson, R.J. McCarty, J.F. Stebbins, Estimating accuracy of ^{17}O NMR measurements in oxide glasses: constraints and evidence from crystalline and glassy calcium and barium silicates, J. Non-Cryst. Solids 358 (2012) 2999.
[49] B.M. Gatehouse, D.J. Lloyd, Crystal-structure of anhydrous potassium carbonate, J. Chem. Soc. Dalton Trans. 1973 (1973) 70.
[50] M.E. Smith, S. Steuernagel, H.J. Whitfield, ^{17}O magic-angle spinning nuclear magnetic resonance of $CaCO_3$, Sol. St. NMR 4 (1995) 313.
[51] H. Koller, G. Engelhardt, A.P.M. Kentgens, J. Sauer, ^{23}Na NMR spectroscopy of solids: interpretation of quadrupole interaction parameters and chemical shifts, J. Phys. Chem. 98 (1994) 1544.
[52] S.K. Lee, J.F. Stebbins, The distribution of sodium ions in aluminosilicate glasses: a high field Na-23 MAS and 3QMAS NMR study, Geochim. Cosmochim. Acta 67 (2003) 1699.
[53] B.C. Schmidt, T. Reimer, S.C. Kohn, H. Behrens, R. Dupree, Erratum to Schmidt B.C., Reimer T., Kohn S.C., Behrens H., and Dupree R. (2000) Different water solubility mechanisms in hydrous glasses along the Qz-Ab join. Evidence from NMR spectroscopy, Geochim. Cosmochim. Acta 64 (2000) 2895.
[54] B.C. Schmidt, T. Riemer, S.C. Kohn, H. Behrens, R. Dupree, Different water solubility mechanisms in hydrous glasses along the Qz-Ab join: evidence from NMR spectroscopy, Geochim. Cosmochim. Acta 64 (2000) 513.
[55] A.M. George, J.F. Stebbins, High temperature ^{23}Na NMR data for albite: comparison to chemical shift models, Am. Mineral. 80 (1995) 878.
[56] J.F. Stebbins, Cation sites in mixed-alkali oxide glasses: correlations of NMR chemical shift data with site size and bond distance, Solid State Ionics 112 (1998) 137.
[57] A. Grund, M. Pizy, Structure cristalline du metasilicate de sodium anhydre, Na_2SiO_3, Acta Cryst 5 (1952) 837.
[58] J.E. Shelby, Thermal expansion of mixed-alkali silicate glasses, J. Appl. Phys. 47 (1976) 4489.
[59] M.E. Brandriss, J.F. Stebbins, Effects of temperature on the structures of silicate liquids: ^{29}Si NMR results, Geochim. Cosmochim. Acta 52 (1988) 2659.
[60] J.F. Stebbins, Temperature effects on the network structure of oxide melts and their consequences for configurational heat capacity, Chem. Geol. 256 (2008) 80.
[61] J.F. Stebbins, Pentacoordinate silicon in ambient pressure potassium and lithium silicate glasses: temperature and compositional effects and analogies to alkali borate and germanate systems, J. Non-Cryst. Solids: X 1 (2019) 100012.
[62] J.F. Stebbins, S. Bista, Pentacoordinated and hexacoordinated silicon cations in a potassium silicate glass: effects of pressure and temperature, J. Non-Cryst. Solids 505 (2019) 234.
[63] H.W. Nesbitt, K.N. Dalby, High resolution O 1s XPS spectral, NMR, and thermodynamic evidence bearing on anionic silicate moieties (units) in PbO-SiO_2 and Na_2O-SiO_2 glasses, Can. J. Chem. 85 (2007) 782.
[64] P. Zhang, P.J. Grandinetti, J.F. Stebbins, Anionic species determination in $CaSiO_3$ glass using two-dimensional ^{29}Si NMR, J. Phys. Chem. 101 (1997) 4004.
[65] J.F. Stebbins, "Free" oxide ions in silicate melts: thermodynamic considerations and probable effects of temperature, Chem. Geol. 461 (2017) 2.
[66] C.R. Masson, Thermodynamics and consitution of silicate slags, J. Iron Steel Inst. 210 (1972) 89.
[67] P.C. Hess, R.B. Hargraves (Ed.), Physics of Magmatic Processes, Princeton University Press, Princeton, NJ, 1980, p. 3.
[68] H.W. Nesbitt, G.M. Bancroft, G.S. Henderson, P. Richet, C. O'Shaughnessy, Melting, crystallization, and the glass transition: toward a unified description for silicate phase transitions, Am. Mineral. 102 (2017) 412.
[69] W.J. Malfait, Comment on "spectroscopic studies of oxygen speciation in potassium silicate glasses and melts", Can. J. Chem. 93 (2015) 578.
[70] H.W. Nesbitt, G.M. Bancroft, Y. Thibault, R. Sawyer, R.A. Secco, Reply to the comment by Malfait on "spectroscopic studies of oxygen speciation in potassium silicate glasses and melts", Can. J. Chem. 93 (2015) 581.
[71] G.E. Brown Jr., F. Farges, G. Calas, J.F. Stebbins, P.F. McMillan, D.B. Dingwell (Eds.), Structure, Dynamics, and Properties of Silicate Melts, Mineralogical Society of America, Washington, D.C., 1995, p. 317.
[72] S.K. Lee, E.J. Kim, Probing metal-bridging oxygen and configurational disorder in amorphous lead silicates: insights from ^{17}O solid-state nuclear magnetic resonance, J. Phys. Chem. C 119 (2015) 748.
[73] N. Kim, R. Bassiri, M.M. Fejer, J.F. Stebbins, Structure of amorphous silica-hafnia and silica-zirconia thin-film materials: the role of a metastable equilibrium state in non-glass-forming oxide systems, J. Non-Cryst. Solids 429 (2015) 5.
[74] N.K. Nasikas, T.G. Edwards, S. Sen, G.N. Papatheodorou, Structural characteristics of novel Ca-Mg orthosilicate and suborthosilicate glasses: results from ^{29}Si and ^{17}O NMR spectroscopy, J. Phys. Chem. B 116 (2012) 2696.
[75] I. Hung, Z. Gan, P.L. Gor'kov, D.C. Kaseman, S. Sen, M. LaComb, J.F. Stebbins, Detection of "free" oxide ions in low-silica Ca/Mg silicate glasses: results from ^{17}O -> ^{29}Si HETCOR NMR, J. Non-Cryst. Solids 445–446 (2016) 1.
[76] S.E. Ashbrook, A.J. Berry, W.O. Hibberson, S. Steuernagel, S. Wimperis, High-resolution ^{17}O MAS NMR spectroscopy of forsterite (α-Mg_2SiO_4), wadsleyite (β-Mg_2SiO_4) and ringwoodite (γ-Mg_2SiO_4), Am. Mineral. 90 (2005) 1861.
[77] S.E. Ashbrook, L. Le Polles, C.J. Pickard, A.J. Berry, S. Wimperis, I. Farnan, First-principles calculations of solid-state ^{17}O and ^{29}Si NMR spectra of Mg_2SiO_4 polymorphs, Phys. Chem. Chem. Phys. 9 (2007) 1587.
[78] F. Angeli, O. Villain, S. Schuller, S. Ispas, T. Charpentier, Insight into sodium silicate glass structural organization by multinuclear NMR combined with first-principles calculations, Geochim. Cosmochim. Acta 75 (2011) 2453.